Article

# Incorporating Backbone Flexibility in MedusaDock Improves Ligand-Binding Pose Prediction in the CSAR2011 Docking Benchmark

Feng Ding[†,‡] and Nikolay V. Dokholyan*[,‡]

[†]Department of Physics and Astronomy, Clemson University, Clemson, South Carolina 29634, United States

[‡]Department of Biochemistry and Biophysics, University of North Carolina at Chapel Hill, School of Medicine, Chapel Hill, North Carolina 27599, United States
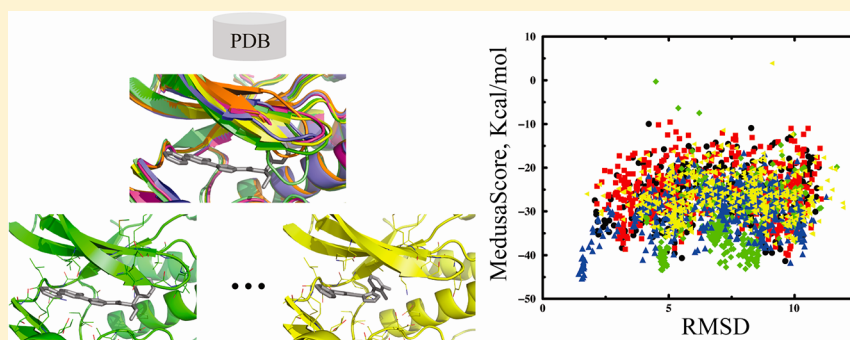
ABSTRACT: Solution of the structures of ligand−receptor complexes via computational docking is an integral step in many structural modeling efforts as well as in rational drug discovery. A major challenge in ligand−receptor docking is the modeling of both receptor and ligand flexibilities in order to capture receptor conformational changes induced by ligand binding. In the molecular docking suite MedusaDock, both ligand and receptor *side chain* flexibilities are modeled simultaneously with sets of discrete rotamers, where the ligand rotamer library is generated "on the fly" in a stochastic manner. Here, we introduce *backbone* flexibility into MedusaDock by implementing ensemble docking in a sequential manner for a set of distinct receptor backbone conformations. We generate corresponding backbone ensembles to capture backbone changes upon binding to different ligands, as observed experimentally. We develop a simple clustering and ranking approach to select the top poses as blind predictions. We applied our method in the CSAR2011 benchmark exercise. In 28 out of 35 cases (80%) where the ligand−receptor complex structures were released, we were able to predict near-native poses (<2.5 Å RMSD), the highest success rate reported for CSAR2011. This result highlights the importance of modeling receptor backbone flexibility to the accurate docking of ligands to flexible targets. We expect a broach application of our fully flexible docking approach in biological studies as well as in rational drug design.

■ INTRODUCTION

One major challenge in computational prediction of receptor−ligand interactions is the large number of degrees of freedom, including receptor backbone and side chain flexibilities, ligand conformational flexibility, and ligand rigid-body motion. Of particular interest is receptor flexibility, which is essential for capturing the receptor conformational changes upon ligand binding, i.e., the induced-fit effect.[1−5] Receptor induced-fit can be limited to the rearrangement of side chains in the binding pocket, or extended to major rearrangement of the backbone, as observed in many kinases.[6] Because of the high dimensionality in describing receptor conformational changes, modeling receptor flexibility is highly challenging and has been one of the foci of recent ligand−receptor docking studies.[3−5,7−11]

Several approaches have been proposed to capture receptor conformational changes. For example, the generation of an ensemble of multiple predetermined conformations has been proposed to model the receptor flexibility. The receptor conformation ensemble can be obtained experimentally by X-ray crystallography under different conditions or by NMR spectroscopy,[12−15] computationally by molecular dynamics simulations,[7,16−19] comparative modeling,[20] or normal-mode analysis.[11,21] In these approaches, the derivation of structural ensembles representing binding-induced receptor conformational change is *decoupled* from the modeling of ligand binding. Each generated structure of the receptor is kept rigid during ligand docking, and receptor conformational flexibility is realized by selecting the optimal poses from ensemble docking in either sequential (independent)[22] or coupled[23] manners. Therefore, the major challenge to overcome in using these approaches is that the predetermined receptor conformational ensemble must encompass significant sampling such

Table 1. Summary Table of the Predicted Ligand—kinase Poses.[a]

Kinase	Ligand index	Ranked by free energy			Ranked by average energy		
		Pose #1	Pose #2	Pose #3	Pose #1	Pose #2	Pose #3
chk1	1	*0.63*	8.46	3.88	*0.63*	8.46	3.90
	3	*0.77*	10.37	9.81	*0.77*	10.37	9.81
	4	*2.03*	10.33	8.86	*2.03*	10.33	8.86
	6	*0.66*	10.68	10.26	*0.66*	10.68	10.26
	18	*1.84*	6.61	3.48	*1.84*	6.61	3.21
	20	5.84	*1.01*	4.09	5.84	*1.01*	4.09
	24	3.84	*2.09*	4.74	3.84	4.74	*2.09*
	27	7.98	*1.98*	8.07	7.98	9.47	*1.98*
	29	9.03	6.91	4.69	9.03	4.69	6.91
	29*	5.90	*2.27*	8.29	5.90	10.00	6.65
	31	6.36	6.60	*1.27*	*1.27*	6.36	6.60
	34	3.50	3.95	9.27	*0.52*	3.50	8.21
	35	*1.80*	8.97	7.89	7.89	4.04	*1.80*
	36	*1.67*	6.26	6.23	*1.67*	4.78	4.60
	37	*1.12*	6.68	5.88	*1.12*	6.68	5.11
erk2	19	*1.49*	4.71	8.31	4.71	5.24	*1.49*
	20	9.18	4.47	*2.10*	3.19	*1.52*	4.94
	22	*2.26*	7.59	6.30	8.45	*2.26*	8.19
	23	8.62	6.25	4.07	7.22	6.19	4.07
	24	3.92	5.42	4.72	5.42	4.72	7.60
	25	7.19	5.74	5.27	5.88	8.30	4.08
	26	6.52	*1.09*	4.98	*1.09*	6.86	6.52
	27	5.22	5.58	6.59	5.58	4.83	6.59
	32	*2.24*	9.35	6.53	9.35	9.89	9.98
	33	3.45	4.38	5.49	4.38	5.49	5.31
	37	10.26	*2.01*	9.88	6.30	9.23	6.96
	39	5.07	*1.23*	5.89	5.89	6.59	5.07
lpxc	2	*1.33*	12.07	7.19	*1.33*	12.07	11.04
	6	*0.96*	2.52	4.67	*1.23*	2.52	5.05
	7	*1.13*	2.59	10.97	*1.13*	2.59	5.42
	7C	*1.44*	2.73	10.98	*1.44*	2.73	11.04
	13	*1.32*	2.69	5.45	*1.32*	2.69	7.21
urokinase	8	*1.16*	1.94	2.28	*1.16*	1.94	2.28
	12	2.57	*0.52*	2.22	2.57	*0.52*	2.22
	14	*1.26*	5.15	6.37	*1.26*	5.15	6.37
	18	4.52	*0.46*	2.71	*0.46*	4.52	2.71

[a]For each ligand—receptor pair, three poses are submitted for the CSAR 2011 exercise. Two ranking methods, according to either binding free energy or the average binding energy (Methods section), were used. The RMSD values smaller than 2.5 Å are highlighted in italic bold font. The cases where none of the top three poses are within 2.5 Å RMSD are in gray shading. *The given smile of ligand #29 for chk1 was different from the actual ligand. We performed *posterior* docking simulations using the same ligand as observed in the crystal structure.

that the ensemble contains favorable receptor conformations for ligand binding.

Alternative approaches have been proposed to simultaneously sample the receptor and ligand flexibilities during docking.[8–10,24–27] For example, protein side chain rotamer libraries, where continuous protein side chain conformational space is modeled by a set of discrete states,[28] have been used to model protein flexibility during docking.[8,10,24–26] Among these rotamer-based approaches, approaches like RosettaLigand[9,26] and MedusaDock[27] extensively sample receptor side chain conformations near the binding pocket during docking, which has been found to increase the prediction accuracy for near-native poses. Specifically, MedusaDock treats ligand conformational flexibility in the same manner as that of protein side chains, with sets of discrete rotamers. The rotamer library of a ligand is generated in a stochastic manner during docking. Benchmark studies of MedusaDock suggested that sampling protein side chain rotamers together with ligand during docking can efficiently capture the receptor induced-fit, as well as improved virtual screening enrichment for flexible targets.[27]

In this study, we incorporate backbone flexibility into MedusaDock in order to blindly predict the ligand-binding poses for the CSAR2011 docking benchmark (www.csardock.org), which includes kinase targets known to be highly flexible.[6,8,29,30] We adopt a simple multiple backbone conformation docking approach, where an ensemble of backbone conformations is selected to capture the backbone changes as observed in receptor structures solved under different conditions, including binding with different ligands. We then sequentially dock the ligand to the predetermined backbone conformations using the flexible side chain/flexible ligand docking suite, MedusaDock. We cluster the top-ranked poses generated from flexible docking to each backbone conformation in order to group structurally similar predictions. We score and rank the clusters in order to select the optimal ligand-binding poses for CSAR2011 predictions. Using the flexible backbone docking protocol of MedusaDock, we were able to predict the near-native poses for 28 out of 35 ligands in the CSAR2011 benchmark, the highest success rate of near-native pose predictions (<2.5 Å RMSD), which highlights the importance of modeling receptor backbone in accurate docking of ligands to a flexible target.

■ METHODS

MedusaDock. We use MedusaDock[27] to generate ligand—receptor binding poses. MedusaDock is a flexible docking method,
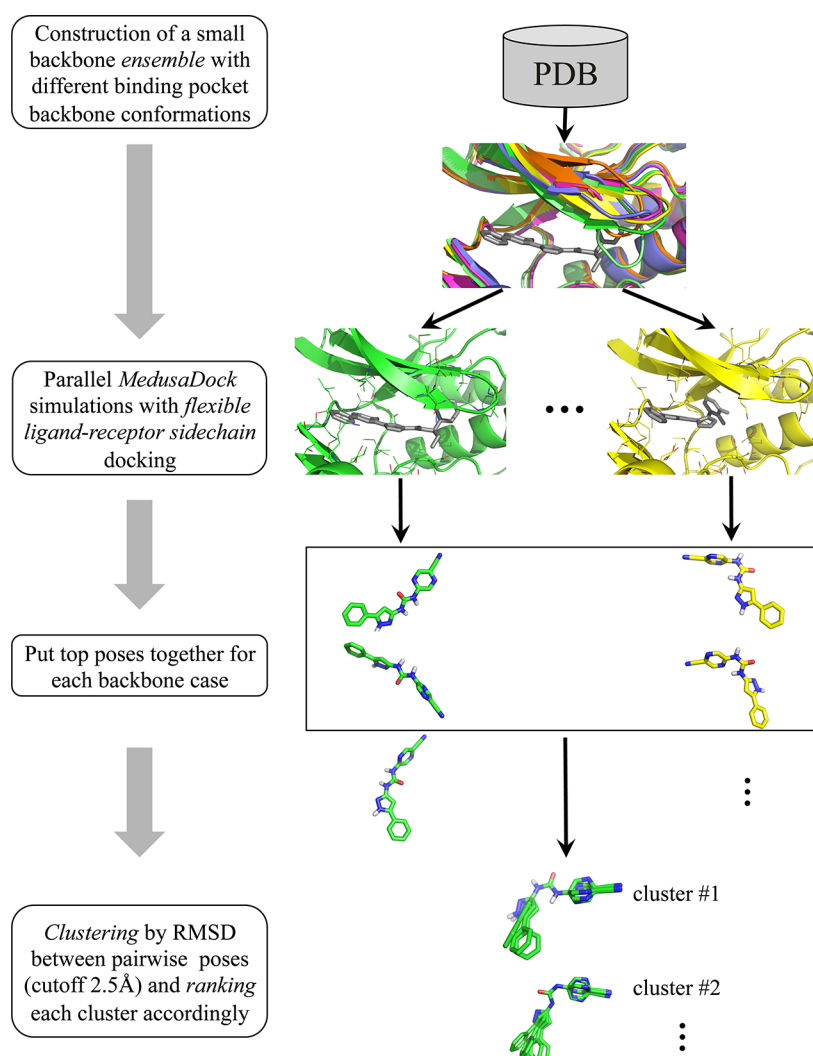
Figure 1. Flowchart of the flexible backbone docking protocol of MedusaDock. The boxes and arrows on the left column summarize the four docking steps (Methods section). The illustrations with protein and/or ligand structures on the right column demonstrate the corresponding steps. Multiple protein backbones in cartoon representation with different colors are selected for independent MedusaDock simulations. The ligands in gray stick are placed in the pocket, where the conformational flexibility of both ligands and receptor side chains (in line representations) are sampled simultaneously. The top poses ranked according MedusaScore are gathered (as shown in the box) for further clustering analysis to group similar poses.

95 where the flexibilities of ligand and receptor side chains are
96 sampled simultaneously. Details of the docking method can be
97 found in ref.[27] Briefly, a ligand rotamer library is generated in a
98 stochastic manner "on the fly". As a result, the sampling of ligand
99 conformations is treated in a unified way, as in the sampling of
100 protein side chains, which are modeled by a discrete set of con-
101 formations, i.e. rotamers.[31,32] The docking protocol is composed
102 of two steps. First, representative ligand conformations are gener-
103 ated by clustering the stochastic rotamer library of each ligand.
104 Each representative ligand conformation is rapidly fitted into a
105 "smoothed" receptor pocket by turning off the van der Waals
106 repulsion between the ligand and the receptor side chains and
107 subsequent rigid-body docking. In the second step, fine-docking
108 is performed from each of the coarsely docked poses, where the
109 binding pose is minimized by iterative repacking of the rota-
110 mers of ligand and receptor side chains as well as ligand rigid-
111 body minimization. In the second fine-docking step, the van der
112 Waals repulsions between ligand and receptor side chains are
113 included. We use the MedusaScore[33] scoring function to guide
114 the docking.

MedusaScore. MedusaScore[33] is a physical force field-
based scoring function that describes the major physical inter-
actions between proteins and ligands, including the van der
Waals interaction (E_{vdw}), hydrogen bonding (E_{hbond}), solvation
(E_{solv}), and electrostatics (E_{es}). The van der Waals interaction
parameters are adopted from the CHARMM19 force field. We
dampen the rapid increase of van der Waals repulsion between
overlapping atoms by linear interpolation of the repulsive
term of the Lennard–Jones potential.[31] We use the distance
and orientation-dependent hydrogen bond model proposed
by Kortemme and Baker.[34] We compute the solvation energy
using the EEF1 implicit solvent model proposed by Lazaridis and
Karplus.[35] The electrostatic interaction is calculated between the
formal charges, including the charged residues of arginine, lysine,
glutamate, and aspartate in proteins, and identified charged
groups in the ligand. We used the distance-dependent dielectric
constant, $\sim r$, to model the screening effect. We also introduce a
solvent-accessibility-dependent weighting coefficient to model
the environmental dependence of the electrostatic interactions.[36]

134 The total MedusaScore describing the binding is the linear sum
135 of all of these energy terms.

$$E = W_{vdw}E_{vdw} + W_{hbond}E_{hbond} + W_{solv}E_{solv} + W_{es}E_{es} \qquad (1)$$

137 Here, the weights (W) were originally trained and deter-
138 mined for describing interamino acid interactions in high-resolution
139 protein structures.[31] Notably, no protein−ligand data was used in
140 the development of MedusaScore,[33] but the scoring function still
141 exhibits remarkable accuracy in both docking pose discrimination
142 and binding affinity prediction. Therefore, MedusaScore features
143 high transferability in both docking and virtual screening.[27]

144 **Backbone Structural Ensemble Selection.** We use the
145 "Sequence Similarity" search functionality included in the pro-
146 tein databank[37] Web site (www.rcsb.org) to identify all solved
147 crystal structures of a protein. Given the reference PDB struc-
148 tures by the CSAR2011 organizers for chk1 (PDB ID: 2e9n),
149 erk2 (PDB ID: 3i5z), lpxc (PDB ID: 3p3e), and urokinase
150 (PDB ID: 1owe) kinases, we identified 62, 10, 4, and 4 solved
151 structures, respectively. Because these ensembles were relatively
152 small and many backbone conformations were very close to each
153 other, we simply aligned all known structures of each kinase and
154 visually identified the representative backbone structures that
155 represented all possible backbone variations in the ligand-binding
156 pocket of those structures using PyMol (www.pymol.org). For
157 large backbone ensembles and also for the purpose of automation,
158 the representative backbones can be selected using clustering
159 analysis.

160 **Clustering.** We cluster the ligand poses by root-mean-square
161 deviation (RMSD). Here, we compute the RMSD between two
162 ligands after aligning the two receptors. During the RMSD
163 calculation, we also consider the symmetry of atoms—where a
164 symmetric rotation does not change the physiochemical property
165 of the ligand, such as benzene ring flipping—by taking the lowest
166 deviation among all such symmetric transformations. We use a
167 hierarchical clustering program, oc (www.compbio.dundee.ac.uk/
168 downloads/oc), to group similar poses using a cutoff distance
169 of 2.5 Å. A hierarchical clustering algorithm iteratively joins the
170 two closest clusters into one cluster according to the distances
171 between two clusters. The "cluster distance" is computed based
172 on all pairwise distances between elements of the two corre-
173 sponding clusters, which can be the minimum, maximum, or the
174 mean of all these values. In this study, we use the mean to com-
175 pute the distance between two clusters.

176 **Ranking of Clusters.** We use two different ranking
177 approaches to rank the clusters. In the first approach, we simply
178 calculate the average MeduaScore

$$\langle E \rangle_c = 1/n_c \sum_i E_i \qquad (2)$$

180 Here, n_c is the cluster size and E_i is the MedusaScore of pose
181 i within a cluster c. In the second approach, we compute the
182 effective free energy of each cluster

$$F_c = \sum_i E_i \exp(-\beta E_i) / \sum_i \exp(-\beta E_i) - k_B T \ln(n_c) \qquad (3)$$

184 Here, β is the reciprocal of $k_B T$, ∼0.6 kcal/mol, which corre-
185 sponds to the thermal fluctuation energy at room temperature
186 (300 K).

■ RESULTS

188 There were four receptor targets in the CSAR2011 docking
189 benchmark exercise, including checkpoint kinase-1 (chk1),

190 extracellular-signal-regulated kinase 2 (erk2), N-acetylglucosamine
191 deacetylase from *Pseudomonas aeruginosa* (lpxc), and urokinase.
192 The sequences and reference structures were given by reference to
193 existing experimental structures: chk1 (PDB ID: 2e9n), erk2
194 (PDB ID: 3i5z), lpxc (PDB ID: 3p3e), and urokinase (PDB ID:
195 1owe). For each target, ligands were provided in the smile format
196 (47 for chk1, 39 for erk2, 16 for lpxc, and 20 for urokinase;
197 www.csardock.org). The participants were allowed to use any
198 information and methods to model the conformations of the bound
199 complexes. For a subset of these ligands (Table 1), the crystal
200 structures of the ligand−receptor complexes were solved and were
201 used to compare with the blindly predicted poses submitted by
202 the participants.

203 **Flexible Backbone Docking Using MedusaDock.** We
204 use MedusaDock[27] to generate ligand-binding poses in a given
205 receptor. MedusaDock models the flexibility of receptor side
206 chains in the pocket but not the receptor backbones (Methods
207 section). To incorporate backbone flexibility for the receptor
208 structures, especially kinases known for large backbone conforma-
209 tional changes upon ligand binding,[6,8,29,30] we develop a simple flexi-
210 ble backbone approach (Figure 1). First, we construct an ensemble
211 of receptor backbone conformations. Because MedusaDock
212 already considers the full receptor side chain flexibility in the
213 binding pocket, which is found to tolerate small backbone varia-
214 tions,[27] we only include a small number of backbone conforma-
215 tions that capture the backbone changes upon ligand binding. We
216 use known receptor structures solved under different conditions
217 to reconstruct the backbone ensemble for each target (Methods
218 section). The backbone ensemble of chk1 includes PDB struc-
219 tures of 2e9u, 2ghg, 2ym4, and 3nle; the ensemble of erk2
220 includes PDB structures of 1tvo, 1wzy, 2ojg, 3i60, and 3sa0;
221 and the lpxc ensemble includes PDB structures of 2ves, 3p3e,
222 and 3u1y. We find significant backbone variation between the
223 various structures of these flexible receptors (Figure 2). We use
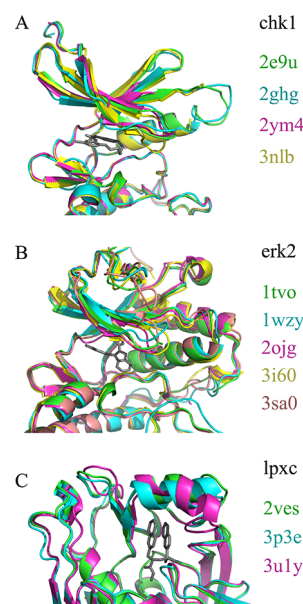

Figure 2. Multi-backbone ensembles for flexible backbone docking.
The backbone structures in cartoon representation with different
colors are selected from the protein databank for different CSAR2011
receptor targets: (A) chk1, (B) erk2, and (C) lpxc. The PDB IDs for
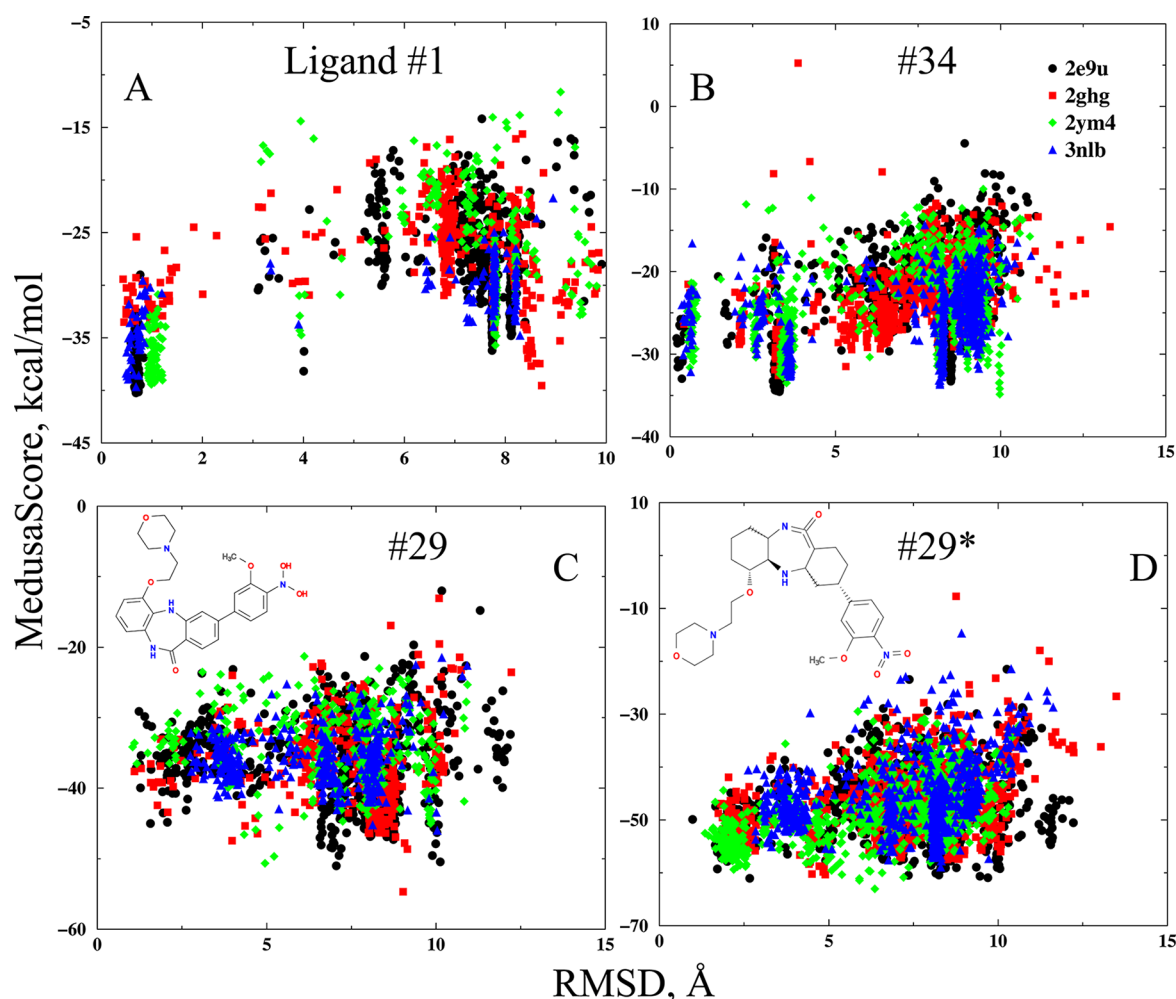the selected backbone structure are colored accordingly.

D

dx.doi.org/10.1021/ci300478y | J. Chem. Inf. Model. XXXX, XXX, XXX−XXX

Figure 3. Scatter plot of MedusaScore versus RMSD for chk1 ligand poses. The symbols with different colors denote docking poses generated with different backbone conformations as shown in the legend. Panel (A) and (B) correspond to docking results of ligand #1 and #34, respectively. (C) The results for the docking of ligand #29 that were initially given, which turned out to be different from the released structure. Panel (D) corresponds to the docking result of the actual ligand #29, #29*. The two chemical structures of ligand #29 are given in the corresponding inserts.

224 only one backbone structure for urokinase (1owe) because all
225 known structures have very similar backbone structures.
226   Second, for each receptor backbone structure, we perform
227 100 independent MedusaDock docking simulations. Depending
228 on the number of degrees of freedom of the input ligand, each
229 MedusaDock run generates several poses[27] and takes on aver-
230 age approximately 3−5 min on an Intel 2.6 GHz Xeon proces-
231 sor. All calculations can be done in parallel. Next, we rank all
232 poses for a given receptor backbone conformation according to
233 MedusaScore (Methodssection; eq 1). We collect the top N_p
234 poses for a given receptor backbone structure and assemble all
235 selected poses $(N_b N_p)$ from N_b backbone structures into a
236 single ensemble for further clustering (Figure 1). Clustering is
237 based on the RMSD between all pairs of poses, the calculation
238 time of which is proportional to $(N_b N_p)^2$. During the CSAR2011
239 exercise, we restricted $N_p N_b$ to approximately 500 total poses. We
240 group similar poses using a hierarchical clustering approach with a
241 cutoff RMSD of 2.5 Å (Methodssection), and each cluster is
242 ranked according to the MedusaScore of poses within the cluster
243 (Methodssection). The centroid poses of the top three clusters
244 were submitted as CSAR2011 blind predictions.
245   **Effective Selection of Native Poses Using Free Energy.**
246 The CSAR2011 organizers allowed submission of more than

247 one set of predicted poses, so that specific hypotheses can be
248 tested. We tested two different approaches to score and rank
249 the pose clusters (Methodssection). In the first approach, we
250 simply score the cluster by the average MedusaScore (eq 2). In
251 the second approach, we compute the effective free energy of
252 the cluster, where the average potential energy is computed as
253 the Boltzmann-weighted average of the MedusaScore, and the
254 entropy contribution is computed as the logarithm of the cluster
255 size (eq 3). We find that the scoring and ranking using the free
256 energy outperforms that by the average energy (Table 1). In the
257 case of free energy ranking, the lowest RMSD of the predicted
258 three poses is within 2.5 Å for 28 out of 35 (80%) targets. The
259 success rate of the predictions computed from the average energy
260 is 26 out of 35. Therefore, scoring and ranking the clusters by the
261 proposed free energy is a more accurate way to select near-native
262 poses.
263   **Docking with Multiple Backbone Conformations**
264 **Enriches Native-Like Poses.** Our simple flexible backbone
265 docking approach is composed of independent MedusaDock
266 docking simulations with a set of predetermined backbone confor-
267 mations, and thus, the number of calculations is proportional to
268 the number of structures used. With ensemble docking, we sacri-
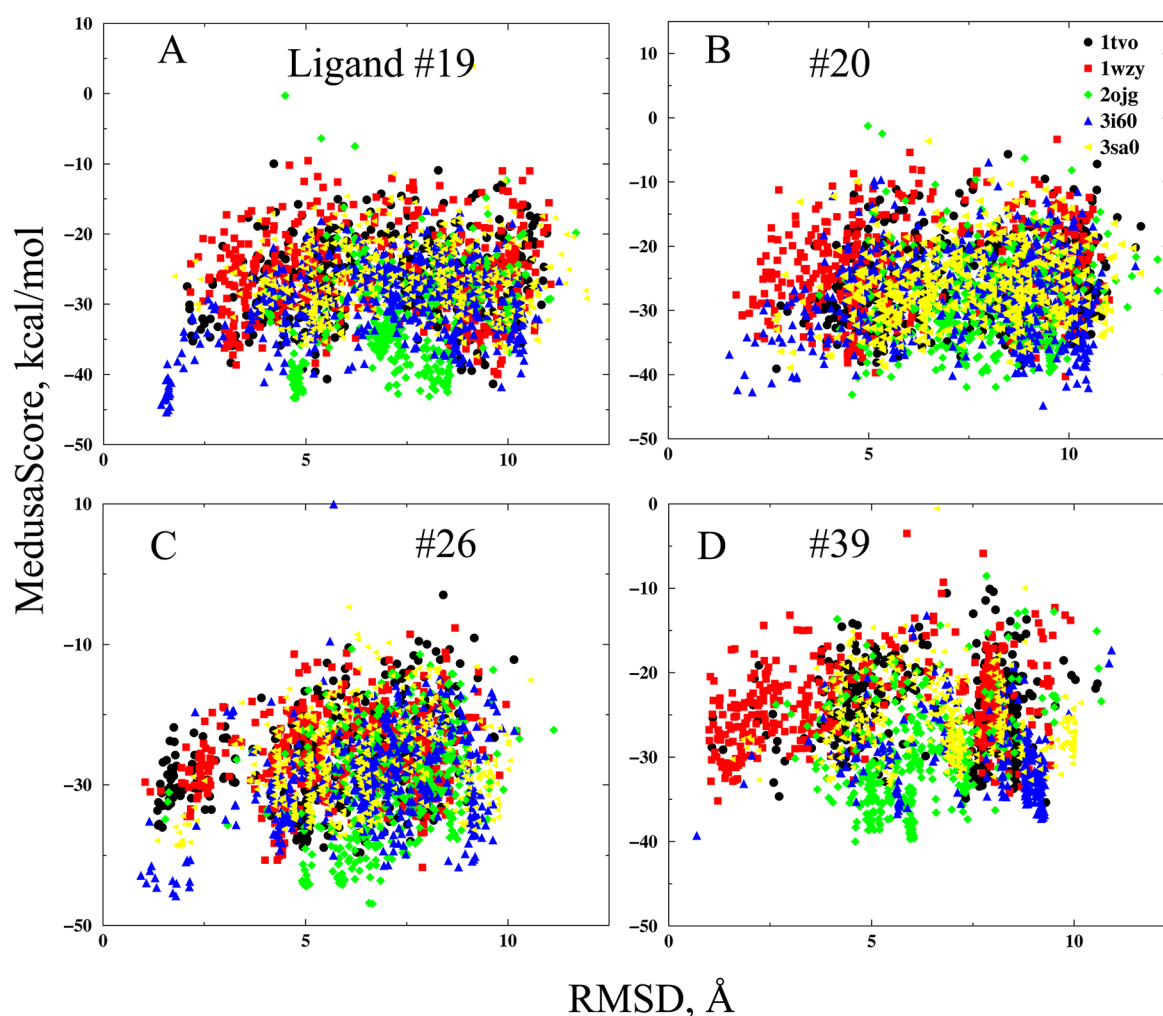269 fice additional required computational time in exchange for

Figure 4. Scatter plot of MedusaScore versus RMSD for erk2 ligand poses. The symbols with different colors denote docking poses generated with different backbone conformations as shown in the legend. Four of the seven success cases are included: ligand #19 (A), #20 (B), #26(C), and #39 (D).

improved prediction accuracy. Next, we discuss the results of docking for each receptor.

chk1. Bound structures have been solved experimentally for chk1 with 14 different ligands (Table 1). Only in two cases (ligand #29 and #34) do our free energy-ranked predictions not succeed in identifying near-native poses. To illustrate the effect of input backbone conformation on pose prediction, we present in Figure 3 the scatter plot of MedusaScore versus RMSD for the poses generated with different backbone conformations. For example, in the case of ligand #1 (Figure 3A), the poses generated from three backbone conformations (2e9u, 2ym4, and 3nlb) feature a funnel-like binding/docking energy landscape, where the native−native poses have the lowest (most favorable) MedusaScores. However, in the case of backbone conformation of 2ghg, the generated near-native poses have higher (less favorable) MedusaScores than other decoy poses. Taken together, MedusaDock simulations with multiple backbones enable the accurate prediction of a near-native pose as the top-ranked pose for ligand #1 (Table 1). For the failed case of ligand #34, near-native poses were sampled for all input backbone conformations but all had higher MedusaScores than the decoy poses (Figure 3B). Interestingly, near-native poses of ligand #34 were top-ranked when utilizing the scoring method with average energy (Table 1). *Additionally, we noticed that the chemical*

structure of ligand #29 in the final released structure is different from that provided by the input smile (inserts of Figure 3C,D). We therefore performed flexible docking simulations for the revised structure of ligand #29 after its final release. Although docking to the backbone of 3nlb did not sample near-native states (Figure 3D), the revised ligand structure enabled sufficient sampling of near-native poses when docked to other backbone structures (Figure 3D), achieving a near-native pose as the second-ranked pose (Table 1).

erk2. Twelve erk2-ligand complex structures have been solved experimentally (Table 1). Our method recapitulated near-native poses for seven out of twelve cases. The relatively low success rate compared to chk1 may be a result of high backbone flexibility, which is manifested even in the success cases (Table 1; Figure 4). For example, near-native poses were sampled by docking only a small number of backbone conformations (e.g., Figure 4A,B) as compared to chk1 (Figure 3). In other cases, the sampled near-native poses did not have clear separation from decoy poses in terms of MedusaScore (Figure 4B,D). However, using the clustering and ranking approach, we are able to select near-native poses from many decoys in the latter cases. These results (Figure 4), as well as those for chk1 (Figure 3), highlight the importance of incorporating multiple backbone conformations in the sampling of near-native poses with low MedusaScores.
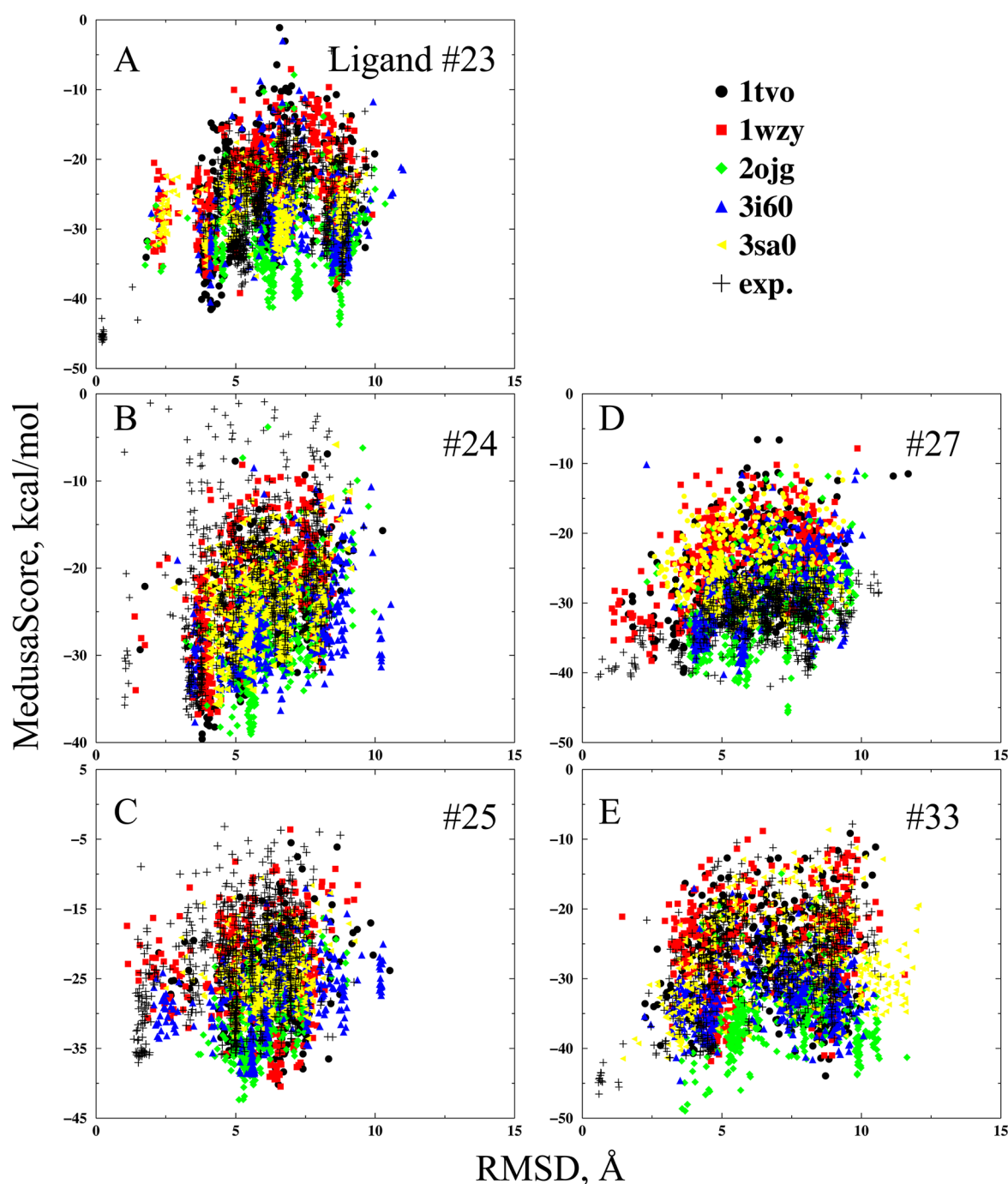
Figure 5. Scatter plot of MedusaScore versus RMSD for erk2 ligand poses. The symbols with different colors denote docking poses generated with different backbone conformations as shown in the legend. Five of the challenging cases are included: ligand #23 (A), #24 (B), #25(C), #27(D), and #33 (E).

In five challenging cases (Figure 5, filled symbols correspond to blind docking results for CSAR2011), the near-native states were either rarely sampled (Figure 5B,E) or sampled but with significantly less favorable MedusaScores than decoys (Figure 5A,C,D). We postulate that the failure to capture near-native states with low MedusaScores is a result of insufficient sampling of backbone conformations in the receptor ensemble. The question is whether docking with the released cocrystallized backbone structure can enrich the near-native poses with low MedusaScores? Therefore, we performed *posterior* MedusaDock simulations with the released backbone conformation. Indeed, the docking with experimentally determined cocrystallized backbone conformations enables the sampling of near-native poses in all challenging cases (Figure 5, plus symbols). If the cocrystallized backbone structures were included in the predetermined backbone ensemble, the near-native poses of these challenging cases could have been selected by our clustering and ranking method as demonstrated by previous examples (Figures 3,4). Hence, the results of these difficult cases suggest that the sampling of backbone conformation in order to capture the backbone changes upon binding of specific ligands remains a significant challenge.

lpxc and urokinase. The lpxc receptor has a zinc ion as the coligand in all existing structures. We include the zinc ion as a

342 fixed moiety during MedusaDock simulation. We recapitulate
343 near-native poses for both receptors (Table 1). In the case of
344 lpxc, all top-ranked poses correspond to near-native poses.

345 ■ **DISCUSSION AND CONCLUSION**

346 In order to model receptor backbone changes upon ligand
347 binding, we develop a simple multibackbone docking approach
348 using MedusaDock. Because MedusaDock is able to model the
349 full receptor side chain flexibility, we construct a relatively small
350 ensemble of protein backbone conformations for the region
351 near the ligand-binding pocket. The flexible side chain docking
352 approach used by MedusaDock can tolerate small backbone
353 changes, as shown in the previous cross-docking benchmark.[27]
354 For this reason, including a small number of backbone confor-
355 mations in the ensemble is most computationally efficient
356 because simulation time is directly proportional to the input
357 number of backbone conformations.

358 The major challenge in ensemble docking is to capture rele-
359 vant backbone changes upon ligand binding within the pre-
360 determined set of backbone configurations. For example, our pre-
361 constructed backbone ensembles for chk1, lpxc, and urokinase
362 (Table 1) are able to capture the corresponding backbone changes
363 upon binding of the given ligands, as suggested by the high
364 success rate of prediction of near-native poses (~100%). How-
365 ever, the prediction rate for erk2 kinase is significantly lower
366 because the backbone structures are not well sampled by the
367 constructed backbone ensemble (Figure 5). In the current study,
368 we have utilized crystallographically determined receptor struc-
369 tures solved in complex with different ligands and under different
370 conditions. Protein structural ensembles derived from solution
371 NMR also provides useful information about protein backbone
372 dynamics,[38] which can be used for the flexible docking approach.
373 With the growing number of protein and protein−ligand com-
374 plex structures deposited into the Protein Data Bank, this approach
375 will have a broad application to drug screening. In cases where a
376 limited number of experimentally solved structures are available,
377 computational modeling of receptor backbone structures can be
378 performed via homology modeling, molecular dynamics, or normal
379 model analysis. The sampling of backbone changes as well as the
380 choice of the optimal number of backbone conformations to use in
381 MedusaDock ensemble docking simulations is a subject for further
382 studies.

383 We group similar poses using a clustering algorithm and
384 develop a free energy-like scoring method to rank clusters of poses.
385 The new score thus considers both the average MedusaScore of
386 each cluster as well as the cluster size in ranking poses (eq 3). We
387 use a Boltzmann-weighted average of MedusaScores within a cluster
388 to compute the final score, where a pose with a lower (more
389 favorable) MedusaScore has a higher weight. The second term with
390 logarithm of the cluster size also favor the large cluster with many
391 similar poses, corresponding to thermodynamic states with large
392 number of microstates and thus high entropy. Our clustering and
393 ranking approach allows us to select near-native poses even when
394 their scores are not obviously separated from those of decoy poses
395 (e.g., Figures 3D and 4B,D). As the result, we are able to predict the
396 near-native poses for 28 out of 35 ligands, which corresponds to the
397 highest success rate of near-native pose predictions (<2.5 Å RMSD)
398 in the CSAR2011 docking benchmark exercise. We expect a broach
399 application of our fully flexible docking approach in pose prediction
400 for both biological study as well as rational drug design.

■ **AUTHOR INFORMATION**   401

Corresponding Author   402
*E-mail: dokh@med.unc.edu.   403

Notes   404
The authors declare no competing financial interest.   405

■ **REFERENCES**   411

(1) Leach, A. R.; Shoichet, B. K.; Peishoff, C. E. Prediction of 412
protein-ligand interactions. Docking and scoring: Successes and gaps. 413
J. Med. Chem. **2006**, *49*, 5851−5855.   414

(2) Sousa, S. F.; Fernandes, P. A.; Ramos, M. J. Protein-ligand 415
docking: Current status and future challenges. *Proteins: Struct., Funct.,* 416
Bioinf. **2006**, *65*, 15−26.   417

(3) Carlson, H. A.; McCammon, J. A. Accommodating protein 418
flexibility in computational drug design. *Mol. Pharmacol.* **2000**, *57*, 419
213−218.   420

(4) Teague, S. J. Implications of protein flexibility for drug discovery. 421
Nat. Rev. Drug Discovery **2003**, *2*, 527−541.   422

(5) Teodoro, M. L.; Kavraki, L. E. Conformational flexibility models 423
for the receptor in structure based drug design. *Curr. Pharm. Des.* 424
2003, *9*, 1635−1648.   425

(6) Schindler, T.; Bornmann, W.; Pellicena, P.; Miller, W. T.; 426
Clarkson, B.; Kuriyan, J. Structural mechanism for STI-571 inhibition 427
of abelson tyrosine kinase. *Science* **2000**, *289*, 1938−1942.   428

(7) Koska, J.; Spassov, V. Z.; Maynard, A. J.; Yan, L.; Austin, N.; 429
Flook, P. K.; Venkatachalam, C. M. Fully automated molecular 430
mechanics based induced fit protein−ligand docking method. *J. Chem.* 431
Inf. Model. **2008**, *48*, 1965−1973.   432

(8) May, A.; Zacharias, M. Protein−ligand docking accounting for 433
receptor side chain and global flexibility in normal modes: Evaluation 434
on kinase inhibitor cross docking. *J. Med. Chem.* **2008**, *51*, 3499−3506.   435

(9) Meiler, J.; Baker, D. ROSETTALIGAND: Protein−small 436
molecule docking with full side-chain flexibility. *Proteins: Struct.,* 437
Funct., Bioinf. **2006**, *65*, 538−548.   438

(10) Nabuurs, S. B.; Wagener, M.; de Vlieg, J. A flexible approach to 439
induced fit docking. *J. Med. Chem.* **2007**, *50*, 6507−6518.   440

(11) Rueda, M.; Bottegoni, G.; Abagyan, R. Consistent improvement 441
of cross-docking results using binding site ensembles generated with 442
elastic network normal modes. *J. Chem. Inf. Model.* **2009**, *49*, 716−725.   443

(12) Barril, X.; Morley, S. D. Unveiling the full potential of flexible 444
receptor docking using multiple crystallographic structures. *J. Med.* 445
Chem. **2005**, *48*, 4432−4443.   446

(13) Sheridan, R. P.; McGaughey, G. B.; Cornell, W. D. Multiple 447
protein structures and multiple ligands: Effects on the apparent 448
goodness of virtual screening results. *J. Comput.-Aided Mol. Des.* **2008**, 449
22, 257−265.   450

(14) Knegtel, R. M.; Kuntz, I. D.; Oshiro, C. M. Molecular docking 451
to ensembles of protein structures. *J. Mol. Biol.* **1997**, *266*, 424−440.   452

(15) Damm, K. L.; Carlson, H. A. Exploring experimental sources of 453
multiple protein conformations in structure-based drug design. *J. Am.* 454
Chem. Soc. **2007**, *129*, 8225−8235.   455

(16) Cheng, L. S.; Amaro, R. E.; Xu, D.; Li, W. W.; Arzberger, P. W.; 456
McCammon, J. A. Ensemble-based virtual screening reveals potential 457
novel antiviral compounds for avian influenza neuraminidase. *J. Med.* 458
Chem. **2008**, *51*, 3878−3894.   459

(17) Soliva, R.; Gelpi, J. L.; Almansa, C.; Virgili, M.; Orozco, M. 460
Dissection of the recognition properties of p38 MAP kinase. 461
Determination of the binding mode of a new pyridinyl-heterocycle 462
inhibitor family. *J. Med. Chem.* **2007**, *50*, 283−293.   463

(18) Karplus, M. Molecular dynamics of biological macromolecules: 464
A brief history and perspective. *Biopolymers* **2003**, *68*, 350−358.   465

(19) Karplus, M.; Kuriyan, J. Molecular dynamics and protein function. *Proc. Natl. Acad. Sci. U.S.A.* **2005**, *102*, 6679−6685.

(20) Fan, H.; Irwin, J. J.; Webb, B. M.; Klebe, G.; Shoichet, B. K.; Sali, A. Molecular docking screens using comparative models of proteins. *J. Chem. Inf. Model.* **2009**, *49*, 2512−2527.

(21) Keseru, G. M.; Kolossvary, I. Fully flexible low-mode docking: Application to induced fit in HIV integrase. *J. Am. Chem. Soc.* **2001**, *123*, 12708−12709.

(22) Cavasotto, C. N.; Kovacs, J. A.; Abagyan, R. A. Representing receptor flexibility in ligand docking through relevant normal modes. *J. Am. Chem. Soc.* **2005**, *127*, 9632−9640.

(23) Huang, S. Y.; Zou, X. Ensemble docking of multiple protein structures: Considering protein structural variations in molecular docking. *Proteins: Struct., Funct., Bioinf.* **2007**, *66*, 399−421.

(24) Kairys, V.; Gilson, M. K. Enhanced docking with the mining minima optimizer: Acceleration and side-chain flexibility. *J. Comput. Chem.* **2002**, *23*, 1656−1670.

(25) Anderson, A. C.; O'Neil, R. H.; Surti, T. S.; Stroud, R. M. Approaches to solving the rigid receptor problem by identifying a minimal set of flexible residues during ligand docking. *Chem. Biol.* **2001**, *8*, 445−457.

(26) Davis, I. W.; Baker, D. RosettaLigand docking with full ligand and receptor flexibility. *J. Mol. Biol.* **2009**, *385*, 381−392.

(27) Ding, F.; Yin, S.; Dokholyan, N. V. Rapid flexible docking using a stochastic rotamer library of ligands. *J. Chem. Inf. Model.* **2010**, *50*, 1623−1632.

(28) Dunbrack, R. L., Jr.; Karplus, M. Backbone-dependent rotamer library for proteins. Application to side-chain prediction. *J. Mol. Biol.* **1993**, *230*, 543−574.

(29) Bahar, I.; Erman, B.; Jernigan, R. L.; Atilgan, A. R.; Covell, D. G. Collective motions in HIV-1 reverse transcriptase: Examination of flexibility and enzyme function. *J. Mol. Biol.* **1999**, *285*, 1023−1037.

(30) Wang, Y. X.; Freedberg, D. I.; Yamazaki, T.; Wingfield, P. T.; Stahl, S. J.; Kaufman, J. D.; Kiso, Y.; Torchia, D. A. Solution NMR evidence that the HIV-1 protease catalytic aspartyl groups have different ionization states in the complex formed with the asymmetric drug KNI-272. *Biochemistry* **1996**, *35*, 9945−9950.

(31) Ding, F.; Dokholyan, N. V. Emergence of protein fold families through rational design. *PLoS Comput. Biol.* **2006**, *2*, e85.

(32) Yin, S.; Ding, F.; Dokholyan, N. V. Eris: An automated estimator of protein stability. *Nat. Methods* **2007**, *4*, 466−467.

(33) Yin, S.; Biedermannova, L.; Vondrasek, J.; Dokholyan, N. V. MedusaScore: An accurate force field-based scoring function for virtual drug screening. *J. Chem. Inf. Model.* **2008**, *48*, 1656−1662.

(34) Kortemme, T.; Morozov, A. V.; Baker, D. An orientation-dependent hydrogen bonding potential improves prediction of specificity and structure for proteins and protein−protein complexes. *J. Mol. Biol.* **2003**, *326*, 1239−1259.

(35) Lazaridis, T.; Karplus, M. Effective energy function for proteins in solution. *Proteins: Struct., Funct., Bioinf.* **1999**, *35*, 133−152.

(36) Matthew, J. B.; Gurd, F. R. Calculation of electrostatic interactions in proteins. *Methods Enzymol.* **1986**, *130*, 413−436.

(37) Berman, H. M.; Westbrook, J.; Feng, Z.; Gilliland, G.; Bhat, T. N.; Weissig, H.; Shindyalov, I. N.; Bourne, P. E. The Protein Data Bank. *Nucleic Acids Res.* **2000**, *28*, 235−242.

(38) Best, R. B.; Lindorff-Larsen, K.; DePristo, M. A.; Vendruscolo, M. Relation between native ensembles and experimental structures of proteins. *Proc. Natl. Acad. Sci. U.S.A.* **2006**, *103*, 10901−10906.